MEMS Scanner for Laser Projection

Steffen Kurth[a], Christian Kaufmann[b], Ramon Hahn[b], Jan Mehner[a], Wolfram Dötzel[b], Thomas Gessner [a,b]

[a] Fraunhofer Institute for Reliability and Microintegration, Dep. MDE

[b] Chemnitz Univ. of Technology, Center for Microtechnologies

1. Introduction

High resolution laser projection demands antagonistic properties of the scanner, as large mirror size, high deflection angle and high scanning frequency[1]. The mirror curvature caused by bending due to mechanical stress of reflection layers and caused by dynamic deformation due to inertia and non perfect stiffness of the mirror can influence the far field spot of the laser beam[2] and should be lower than 1/10 of the smallest used wavelength. A design with a higher mirror thickness, proposed e.g. in Refs. [3,4] is the most common way to overcome this problem but it leads to higher inertia, stiffer torsion beams and to higher driving force in consequence.

In the following, a micromachined resonant scanner usable for horizontal deflection of the laser beam in a projection display is described and its analysis is reported. The approach followed here is based on a two degrees of freedom resonator. The magnitude amplification occurs at the resonant frequency of the second resonant mode. The relatively low deflection of driving plate in comparison to the mirror makes a very small electrode gap size possible. It leads to a high electrostatic force and low influence on the Q-factor of the used resonant mode caused by the air flow in the electrode gap.

2. Design

The device (Fig. 1) consists of a circularly shaped silicon plate which is suspended by torsion beams in the center of an elastically suspended driving plate. The moving part of the scanner basically consists of two mechanically coupled resonators. The inner resonator acts as scanning mirror. The outer resonator is used to drive this mechanical system. A resonator with two rotational degrees of freedom is arranged in this way. The rotation axes of mirror and driving plate are the same. A supporting part made of glass carries two electrodes in the region of the driving plate. A voltage between the electrodes and the driving plate produces electrostatic torque primarily onto the driving plate.

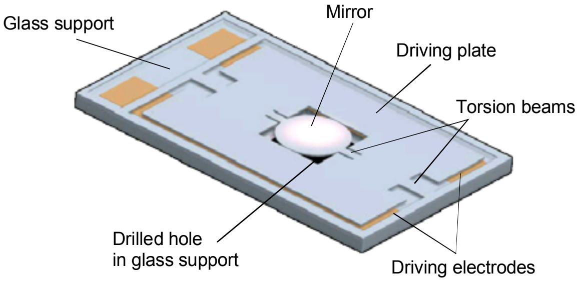

Fig. 1: Outline of the scanner

3. Modeling and simulation

3.1 General aspects

Neglecting motion in other direction than rotation concerning the axis of torsion beams, the mechanical system can be generally mathematically described by the corresponding differential equation of motion. The two angular eigenfrequencies are given by the square roots of the eigenvalues:

$$2\pi\ f_{0i} = \sqrt{Eigenvalue\ \left(\mathbf{J}^{-1}\ \mathbf{K}\right)} \qquad (1)$$

whereby **K** denotes the stiffness matrix and **J** denotes the matrix of inertia. The ratio of the amplitudes of each resonant mode is given by the eigenvector of the corresponding eigenvalue. After substitution of the stiffness and mass moments of inertia by ratios of both mass moments of inertia $A = J_1/J_2$ and of both rotational rigidities $B = k_1/k_2$ respectively, the ratio of both elements of the eigenvector corresponding to the 2nd eigenfrequency can be expressed by

$$\frac{\alpha_{01}}{\alpha_{02}} = \frac{2\,B}{A - B + A\,B + \sqrt{-4A\,B + \left(A + B + A\,B\right)^2}}\ . \qquad (2)$$

It reflects the ratio of angular deflections of mirror and driving plate illustrated in Fig. 2.
One can see that the deflection of mirror is much higher than the deflection of driving plate. In consequence, the deflection of the mirror is amplified in respect to the deflection of the driving plate 25…200 times within the boundaries of the diagram. The negative sign of the ratio indicates a paraphase motion of mirror and driving plate at the 2nd eigenfrequency. One can see that *A* strongly influences the amplification whereas the amplification is less sensitive regarding *B*.

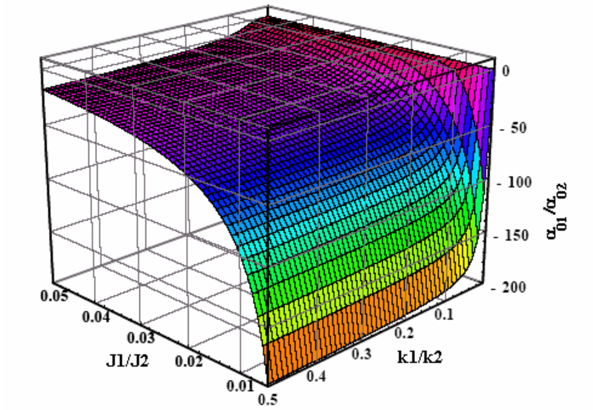

Fig. 2: 3D plot of the dependency of deflection amplification on the ratio of mass moments of inertia and of stiffness

The diameter of the mirror plate with D = 2.2 mm, the maximum mechanical angular deflection of $\alpha_{01} \geq 5°$ and the scanning frequency $f_{scan} = 48\,kHz$ are the main constrains for design. A suitable design of the properties of the two degrees of freedom resonator leads to a significant amplification of the oscillation of the mirror in respect to the oscillation of the driving plate. The first resonant mode is a rotation of both plates with nearly the same magnitude at a frequency of 5.5 kHz. The second mode with paraphase deflection at 24 kHz shows the amplitude amplification. We decided for 280 µm thickness of the mirror and driving plate in order to achieve sufficiently low dynamic mirror curvature. Thus the values of mass moments of inertia are determined by geometry and specific weight.

3.2 Damping

Damping moments acting on the mirror and on the driving plate originate from the energy dissipation within the surrounding air. For analysis of damping we consider two different parts of this space. The first one with main energy dissipation is the space in between the driving plate and the electrodes which is characterized by a viscose air flow. The other part comes from the flow above the driving plate and around the mirror plate. We analyzed the second part experimentally and included the damping in the model. The calculation of damping and the experimental procedure to determine the part caused by air flow above the mirror is explained within Ref. 5 in detail.

3.3 Analysis in frequency domain

An analysis of the mechanical system in frequency domain gives the magnitude and phase of the angular deflection of the mirror and of the driving plate as to be seen within Fig. 3. A voltage of 400 V_{pp} superimposed by 200 V_{dc} has been assumed for driving. One can clearly see both resonant peaks. Mirror plate and driving plate oscillate with nearly equal deflection magnitude and same phase at the first resonant frequency (5.5 kHz). The second resonant peak indicates a substantially higher Q-factor compared to the 1st one and a magnitude amplification of 53 at this frequency. It equals the ratio of the eigenvalues of characteristic equation without damping. The theoretic analysis gives a motion in paraphase of mirror and driving plate and a phase shift 1.5 π regarding the driving torque. The maximum mechanical deflection is calculated to be ± 5.7 deg.

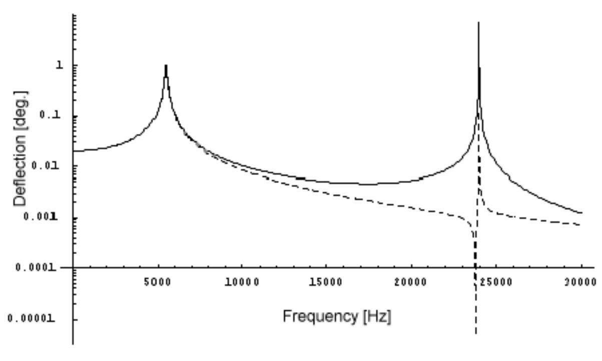

Fig. 3: Calculated magnitude of angular deflection of mirror and of driving plate

4. Results

4.4 Flatness of mirror surface

The aluminum reflection layer and the combination of silicon and glass with different thermal expansion coefficients are two main reasons for mirror and chip deformation induced by mechanical stress. The topography of mirror, driving plate and torsion beams has been measured using a customized phase shift interferometer. The circular mirror surface is very smooth and flat. Its deviation from plane is less than ±15nm and lower than λ/10 in respect to the wavelength of visible lasers. (Fig. 4).

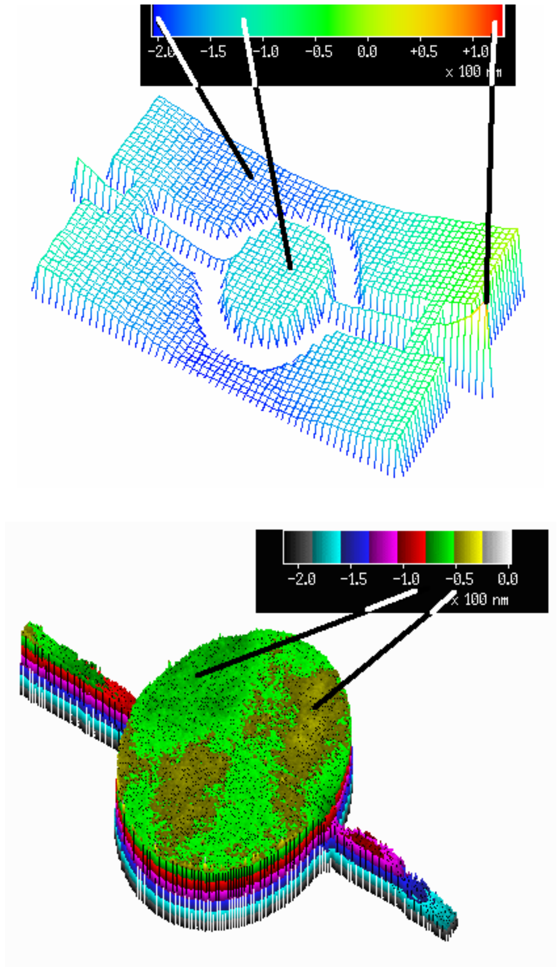

Fig. 4. Surface profiles of driving plate and mirror (upper image) and of the mirror (lower image) measured by a phase shift interferometer

4.5 Scan angle and frequency behavior

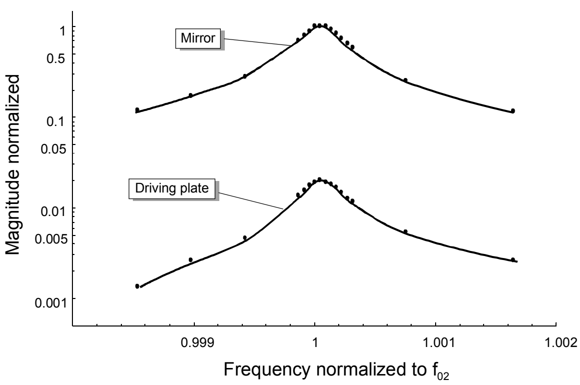

Fig. 5. Measurement result of deflection angle in dependency of frequency of the driving voltage

Applying a voltage of $380V_{pp} + 190V_{dc}$ with the frequency corresponding to the frequency of second resonant mode results in a mechanical deflection of ± 5.5 degrees (22 deg measured scan angle). The mechanical Q-factor is 5100 operating the scanner at atmosphere. It is expected that the high Q-factor leads to low jitter of scan angle. The mechanical bandwidth is approximately 5 Hz (see Fig. 5).

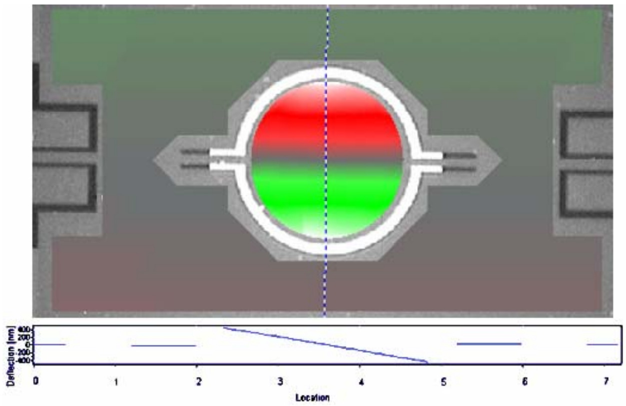

Fig. 6. result of measurement of dynamic behavior by Laser Scanning Vibrometer.

Fig. 6 shows a result of deflection measurement by a Laser Doppler Scanning Interferometer. It clearly shows the paraphase motion of mirror and driving plate and the amplification of the mechanical deflection. The theoretically predicted amplification of the deflection by a ratio of 53, the Q-factor, the resonant frequencies and the maximum mechanical deflection angle agree very well with the measured values.

REFERENCES

1. H. Urey, D. W. Wine, T. D. Osborn, *Optical performance requirements for MEMS-scanner based microdisplays* , Proc. of SPIE Vol. 4178, pp. 176-185.
2. H. Schenk, P. Dürr, D. Kunze, H. Lakner, H. Kück, *Design and modelling of large deflection micromechanical 1D and 2D scanning mirrors*, Proc. of SPIE Vol. 4178 (2000), pp. 116-125.
3. R. A. Conant, J. T. Nee, K. Y. Lau, R. S. Muller, *A flat high-frequency scanning micromirror*, IEEE Solid State Sensors and Actuator Workshop, Hilton Head, June 2000, pp. 6-9.
4. H. Urey, F. DeWitt, P. Lopez, J. Tauscher, *MEMS raster correction scanner for SXGA resolution retinal scanning display*, Proc. of SPIE Vol. 4985, pp. 106-114.
5. S. Kurth, C. Kaufmann, R. Hahn, J. Mehner, W. Dötzel, T. Gessner, A novel 24 kHz resonant scanner for high resolution laser display, to be published in Proc. of SPIE, Vol. 5721 (2005)